

**STEEL CATENARY RISERS – ALLEGHENY OFFSHORE VIV MONITORING CAMPAIGN AND  
LARGE SCALE SIMULATION OF SEABED INTERACTION**

*Paolo Simantiras, Neil Willis*  
2H Offshore Engineering Ltd  
Woking, Surrey, UK

## ABSTRACT

This paper deals with two design aspects for deepwater steel catenary risers (SCR's) that have been high on the list for research activity in recent years – vortex induced vibration (VIV) and seabed interaction at the touchdown point (TDP). The work was performed as part of the STRIDE JIP.

*VIV Monitoring Campaign.* The Allegheny gas export line was instrumented during riser installation in August 1999 with 12 2H accelerometer units. The SCR has an outer diameter of 12.75" and is fitted with strakes over the top 580 ft. The Allegheny field is situated in 3255 ft (992 m) water depth in the north of the Gulf of Mexico (GoM). Currents up to ~2 knots were monitored by acoustic Doppler current profiler (ADCP) during the logging period. The paper describes the monitoring programme and data analysis techniques, and gives some indication of the measured response.

*TDP Test Programme.* A test programme was performed that involved a 360-ft long 6-inch diameter steel pipe that was hung as a catenary across the soft seabed of a tidal harbour that had seabed properties similar to those of the deepwater Gulf of Mexico. The top end of the pipe string was then actuated with PLC controlled wave and vessel drift motions to simulate a spar platform in 3,300-ft water depth, both in line and transverse to the SCR plane. Tests were performed at high and low tide. Investigations included:

- how vessel wave and drift motions can cause increased riser wall stresses at the TDP due to soil suction effects;
- the effect of seabed loading history

"Riser" wall stress increases were attributed to soil suction effects causing local high bending moments. The higher levels of stress delta were seen for a sudden riser excursion following a long period at rest, such as might be caused by vessel drift after a failed mooring line. If instead the vessel excursion was caused by a building storm, simulated wave action at the vessel was seen to break down the suction effect dramatically.

**KEY WORDS:** Steel catenary riser (SCR), vortex induced vibration (VIV), touchdown point (TDP)

## VIV MONITORING CAMPAIGN

### VIV - Introduction

Major research efforts have focused on VIV and suppression devices for slender tubulars subject to uniform flow along their length, for instance for vertical drilling risers. For catenary risers, the flow incidence is generally variable along the component axis and the description of the interaction between the fluid and the tubular component is extremely difficult. Velocity gradients can generate a multi-modal excitation where the tubular presents both excited stretches and damping zones (Griffin, 1985; Humphries, 1998; Vandiver, 1985,1993), and suppression devices that are satisfactory for certain excitation regimes may fail under different conditions (Jacobsen et al., 1996).

There was therefore considered to be a requirement to better understand the effect of VIV due to flow over inclined risers, and the ability of suppression devices under these conditions. An opportunity was taken to put accelerometer logger units onto the Allegheny gas export SCR in August 1999, a mini-TLP development well-placed for significant loop current eddy events.

### VIV - Riser and Monitoring System Description

*Allegheny SCR.* The Allegheny field is situated in 992 m water depth in the north of the Gulf of Mexico. Now operated by Agip Petroleum, it makes use of a SeaStar mini-TLP platform. The two export lines, oil and gas, were installed during July-August 1999 by the McDermott DB50 via J-lay. Both lines are simple catenary risers.

The instrumentation was installed on the gas export line, details of which are given below:

#### GAS EXPORT LINE

outer diameter	12.75" (0.3239 m)
wall thickness	0.688" (17.5 mm)
departure angle	12°
hang-off position	25 m below MWL

The gas export line is orientated as shown in Figure 1.

The riser is fitted with 3-start helical strakes over the top 580 ft with the following characteristics:

#### STRAKES

height	0.16 D
pitch	15.0 D

*Environmental data.* The environmental data for the site has been provided by British Borneo Exploration / Agip Petroleum. Current data was logged from November 1999 by a deepwater acoustic Doppler current profiler (ADCP) at the Attwood Hunter drill rig working at Allegheny.

*Data loggers.* In order to monitor the VIV response, the Allegheny gas export line was fitted with 12 triaxial linear accelerometer 2H Data Loggers (Figure 2). The data logger units were attached to the riser through holders made from high strength 'E' glass laminate. The holders were strapped to the riser using titanium straps and will remain in place for the life of the riser.

The instrumentation was fitted as follows:

- one data logger on a pup joint above the riser hang-off position to monitor vessel motions;
- eight data loggers placed along the top 850 ft of the riser, spanning the straked and unstraked areas of the mid-water riser;
- three data loggers placed near to the nominal riser touchdown point (TDP).

In particular, the position of the loggers along the riser is reported in Table 1 and depicted in Figure 3.

The core of each logger is a set of three monolithic IC accelerometers, measuring  $\pm 5g$  in three mutually orthogonal directions. These sensors were mounted inside the pods in such a way that, when the loggers were fitted to the riser, their measuring directions were aligned with the riser local axis directions (Figure 4). Prior to installation, all the loggers were synchronised with the same PC clock, which was constantly updated by radio link to an atomic clock transmission. Sample rate was 10 Hz, and data was logged for 20 minutes every 6 hours, at 00:00, 06:00, 12:00 and 18:00, and stored within the built-in memory.

Of particular interest during the logging period, a significant eddy was shed from the loop current that produced currents at Allegheny up to ~2 knots.

Data was gathered from the time the loggers were installed on the riser (19 August 1999) until the memory was full (10 January

2000). The loggers were retrieved by ROV in March 2000, and replaced with a second set.

*Downloaded data.* Approximately 197 MB of data was downloaded from each data logger, giving a total of 2.36 GB. All loggers downloaded properly and all checks indicated that the data was of good quality.

#### VIV - Analysis Methodology

The post-processing of the data is carried out through specifically developed PASCAL and MATLAB procedures. For the current purposes, the MATLAB Signal Processing Toolbox is used to access the filter design facilities.

The Pascal procedure reads the raw accelerometer data of each logger, corrects the signals by the calibration curves and temperature, and splits the logger related data file into smaller files, each relative to an individual test.

The Matlab procedure processes the accelerometer data of each data block and evaluates, by successive integration, the velocity and displacement times histories, as well as the fast Fourier transform (FFT) of accelerations, velocities and displacements. As the accelerometer readings generally have a non-zero "running" mean value and due to the errors introduced by describing the signals with samples, the data is properly filtered to avoid the corresponding displacement time histories being characterised by huge drifts. User activated options are available to visualise on screen, print and/or store into file any of the processed variables.

*Frequency Domain Analysis.* The Fourier analysis is based on Fourier's theorem that every periodic signal can be decomposed in a series of harmonic functions. The discrete Fourier transform, or DFT, is the primary tool of digital signal processing. The Fast Fourier Transform (FFT) is a method for computing the DFT with reduced execution time.

Every digital signal analysis method can only deal with a limited section of the time signal. The signal outside this section is always assumed to be a periodic continuation of that section. The length  $T$  of the analysis interval determines the basic frequency:

$$f_b = \frac{1}{T} \quad (1)$$

If, as generally the case, the time signal contains frequencies which are not an integer multiple of that frequency, these frequencies will not be identified as sharp spectral lines but smeared to several lines. This is called the leakage effect. The choice of a well-suited window vector can reduce this effect, but it will also lead to undesirable side effects for the analysis, like widening of the main lobe.

*Kurtosis.* Screening of the acceleration data for significant events is performed by using kurtosis (Vandiver, 2000), a statistical parameter defined as:

$$K = \frac{\langle acc^4 \rangle}{\langle acc^2 \rangle^2} = \frac{(\overline{acc - \overline{acc}})^4}{(\overline{acc - \overline{acc}})^2} \quad (2)$$

where  $acc$  is the acceleration time series and overscore denotes time average.

Kurtosis assumes a value of 1.5 for a sinusoidal process, as is typical of single mode lock-in events, and a value of 3.0 for a Gaussian process, as is typical of multi-frequency random vibration.

A 128 point window and a 50% overlapping have been used in the analysis.

*Root Mean Square Displacement.* Even if the acceleration time histories are the fundamental ones for the prediction of the stresses and the fatigue damage, amplitudes are useful for implying modal response, damping levels, and for benchmarking software to some extent.

Given the acceleration time histories, the aim is to reconstruct the displacement histories by double integrating the acceleration signals.

Inconveniently, integration has the characteristics of a low-pass filter with a gain that goes to infinity as the frequency goes to zero. This leads to the undesirable expansion on low frequency noise in the integration process. That is, after integration, low frequency noise dominates the velocity signal, and leads to unacceptable integration error. To avoid the problem, a high-pass filter is required to cut-off the low frequency noise before integrating. Analogously, the same problem arises when integrating the velocity signal to obtain displacement. That is, when carrying out the double integration in the time domain, the acceleration signal has to be filtered three times, once before each of the two integrations and once after the second integration. The obtained displacement time history is clearly strongly dependent on the assumed cut-off frequency for the high-pass filter. The cut-off frequency of such high-pass filter has to be carefully selected, as it has to be high enough to eliminate drift but also low enough to not cut any phenomenon significant frequency.

Due to the intrinsic difficulties of such a proper selection, an alternative procedure is considered (Chung, 1987), carrying out the integration in the frequency domain. This may not completely eliminate the difficulties of a proper cut-off frequency selection, but has the advantage that such selection can be done after the double integration is performed.

At first, the spectral density of the acceleration is evaluated by using the Welch's method (Welch, 1967), associated to a 1024 point Hanning window and a 50% overlap rate.

The spectral density of the displacement is consequently found by:

$$S_{dpl}(f) = \frac{S_{acc}(f)}{(2\pi f)^4} \quad (3)$$

Then, the root mean square (rms) displacement can be evaluated as:

$$dpl_{rms} = \sqrt{\int_0^{+\infty} S_{dpl}(f) df} \quad (4)$$

Filtering the acceleration signal with an ideal high-pass filter with a given cut-off frequency  $f_{cut-off}$ , the corresponding rms displacement results:

$$dpl_{rms}(f_{cut-off}) = \sqrt{\int_{f_{cut-off}}^{+\infty} S_{dpl}(f) df} \quad (5)$$

As the spectrum of a signal sampled at a frequency  $f_s$  spans up to the Nyquist frequency,  $f_N = f_s / 2$ , the above expression reduces to:

$$dpl_{rms}(f_{cut-off}) = \sqrt{\int_{f_{cut-off}}^{f_N} S_{dpl}(f) df} \quad (6)$$

This relationship allows evaluation of the rms displacement as a function of the cut-off frequency of the high-pass filter.

The proper cut-off frequency can now be selected from the relevant graph as the lowest frequency marking the transition of

the curve slope to an extreme value, which is clearly an effect of the amplified noise contribution, Figure 5.

#### VIV - Results

Full results from the test programme are restricted to STRIDE ticket holders, though some have been approved for inclusion within this paper.

At first, attention was focused on Logger 10 which, located at a water depth of ~339 m, is the deepest of the mid water loggers.

A screening of the data for significant events has been performed by evaluating the kurtosis of acceleration and looking for time intervals where its value drops below 2.

However, it has been found that, for the current analysis, a more appropriate screening is given by looking at the root mean square displacements.

The amplitude spectrum of acceleration has also been evaluated through the Welch's method (Welch, 1967).

Successively, the above analysis has been extended to all loggers. Then, for each test, the rms displacement, the maximum peak frequency of the acceleration spectrum has been plotted along the riser axis.

From the examination of such spanwise correlation plots, the response of the Allegheny gas export line can be classified into the following four classes:

- <C1> : small amplitude response;
- <C2> : vessel motion induced response;
- <C3> : VIV induced response;
- <C4> : "mixed" response.

Figure 6 provides a summary of the response vs. time and in relation to the current speed and direction at 70 m water depth.

#### VIV - Conclusions

The Allegheny data has proved that SCRs are also subjected to VIV response. However, VIV response was less than expected, both in terms of response amplitude and occurrence. The reasons for this are still under investigation, current thoughts are:

- Strakes more efficient than expected
- Coupling of the "in-plane" and "out-of-plane" response of the SCR
- Current directionality through the water column.

Indeed, some of the VIV plots from Allegheny showed clear coupling of in-plane and out-of-plane VIV response of the SCR. This highlights the shortcoming of the prediction codes currently available, which predict separately in-plane and out-of-plane response of SCRs.

#### VIV - Future Work

Tests to investigate the influence of flow direction on the VIV response of an SCR will be carried out within STRIDE Phase 4 (STRIDE, 2000). An SCR differs from a vertical riser having preferred vibration directions orthogonal to the riser curvature plane. The tests will be executed at MARINTEK facilities in Trondheim, Norway, and will be focusing on the coupling of in-plane and out-of-plane VIV response.

## TDP TEST PROGRAMME

### TDP - Introduction

Deepwater oil and gas fields usually have seabeds of soft clay. ROV surveys of installed catenary risers have shown deep trenches cut into the seabed beyond the TDP, apparently caused by the dynamic motion of the riser.

Storm and current action on a deepwater production vessel can pull the riser upwards from its trench, or laterally against the trench wall. The suction effect of the soft seabed on the riser, coupled with trench wall interaction, could cause an increase in the local riser stresses by causing tighter riser curvatures or higher tensions than those predicted ignoring these effects.

As part of the STRIDE III JIP, 2H Offshore Engineering conducted a test programme to investigate the effects of a deepwater seabed on catenary riser response and wall stresses. The objective was to assess the importance of such seabed/riser interaction, and to produce finite element (FE) analysis techniques to match the real response as necessary.

### TDP - Pre-Analysis

Initially, FE analysis was performed to predict the motions of a 6-inch diameter SCR attached to a spar platform in 3,300-ft water depth in the Gulf of Mexico, Figure 7. Day-to-day and extreme environmental load-sets were applied using FE program Flexcom-3D (MCS, 1999), including wave and drift effects both in and out of the riser plane. The riser motions near the seabed were recorded as output from these analyses, and in particular the local velocity of the riser as it peels away from the seabed.

A second FE model was then used to simulate the planned test set-up, comprising a welded steel pipe that represented the bottom 360-ft of the full-scale riser (Figure 8). The model simulated a linear actuator at the top end, and the actuation cycles were varied within the FE model until similar SCR motions were obtained for the reduced size model as for the full depth case. These actuator motions were then used in the design of the actuator rig for the intended tests, allowing a deepwater riser to be simulated at cut-down scale.

### TDP - Test Set up

The test programme was conducted at a harbour location in the west of England, where the seabed was known to have properties similar to a deepwater Gulf of Mexico seabed - soft clay, typically 3 to 5 kPa undrained shear strength, with a naturally consolidated shear strength gradient below the mudline. The sea current velocity in the test area as the harbour filled or emptied was almost negligible, and any trenches formed by the testing remained unchanged over numerous tide cycles.

A 360-ft long 6-in diameter welded steel "riser" was suspended from an actuator on the harbour wall, Figures 8 and 9, and run out across the seabed to a set of mud anchors. The seabed over this area was flat and undisturbed, and careful probe tests were done to check that there were no hidden obstacles below the mudline.

The test set-up allowed the use of a number of virgin test corridors at the flattest part of the harbour seabed. It was important that these corridors were undisturbed before the testing. To ensure this, the riser was floated to the various positions using temporary buoyancy, then the outgoing tide allowed it to settle onto the seabed.

The riser was fixed at its top end to an actuator unit. This comprised a heavy-duty truss frame with a 10-ft linear ball screw driven from one end by a motor with displacement feedback control via PLC (Figure 10). The riser was attached to the ball screw nut. The linear screw could be swivelled to operate in

vertical or horizontal directions to provide the prescribed motions accurately to the top end of the cut-down riser, and produce the vertical and lateral pipe motions being sought at the seabed. This meant linear ramps, simulating vessel drift, and sinusoidal motions of different amplitudes and frequencies, simulating wave loading. In addition the whole actuator frame was designed to move on a set of 10 m long rails, simulating a large transverse excursion of the vessel and pulling the riser laterally from its trench while pipe stresses were monitored.

The primary instrumentations comprised full bridge strain gauge sets welded at 13 axial positions along the riser, spanning the dynamic TDP area (Figure 8). Each position provided vertical and horizontal bending strain on the pipe. In addition, a triaxial accelerometer unit was mounted just above the nominal TDP, there were tension load cells top and bottom of the pipe string, and shear force measurement at the connection between pipe and actuator. All instrumentation was hardwired to a multi-channel logging station able to monitor in real-time at 40 Hz.

### TDP - Results

Full results from the test programme are restricted to STRIDE ticket holders, though some have been approved for inclusion within this paper.

Figure 11 shows strain gauge data from a spar fast drift simulation "near-to-far". This simulation means moving the top of the test riser 7 ft vertically at 0.1 m/s, and simulates the spar drifting 80 ft in 22 seconds in the plane of the SCR and pulling the riser tauter. The start and end of the traces correspond to the static bending moments at near and far (here negative bending moment corresponds to a sagging bend in the riser). However, it is the transient part of the traces that is of particular interest here. Only a selection of the 13 strain gauge stations is shown for clarity, but it can be seen that some of the traces show a clear peak as the riser lift-off point passes through that strain gauge position. The clearest proof that these peaks were due to soil suction was to follow a pull up test with a riser lay-down, "far-to-near" at exactly the same rate as the lift and to compare the traces. The pick-up sees the suction effect, the laydown does not. This can be seen in Figure 12, where the pick-up and laydown curves for three of the gauge stations are overlaid.

The suction peak was seen to move through the riser TDP at ~1 m/s. It grew and then faded as it traversed the 20 m dynamic riser length, and the strain gauge position with the highest suction peak could then be given closer attention. Figure 13 shows an example of this. For this test the pipe was in a backfilled trench and had been allowed to consolidate the soil overnight. The test then simulated the fast drift as before, and the strain gauge with the highest peak is plotted. Examination of the recorded tensions did not show a significant difference between the suction and non-suction cases, and it seems that the riser stresses are bending dominated in this area.

Tests were also conducted on a simulated rigid seabed, by actuating the riser on top of a steel grid walkway placed on the harbour floor. These tests did not show the suction peak identified in Figure 13. Figure 14 shows bending moment traces from strain-gauges at different riser positions along the test pipe. It can be seen that the lift and lay-down strain gauge curves are almost identical. This was as expected and indicated that the suction peaks were due to soil suction, and not a result of the actuation system or hysteresis/inertia effects.

### TDP - Conclusions

It is important to emphasise that the conclusions relate to the set up simulated and may not apply to other seabed types or riser configurations:

- A sudden vertical displacement of a catenary riser at its touchdown point (TDP) after a period at rest could cause a peak in the bending stress that travels along the riser. Such an event may occur from a vessel failed mooring line, or a move away for drill rig access.
- Once the seabed/riser interface has been disturbed, subsequent seabed/riser interface contacts produce less suction effect.

### TDP - Future Work

The significance of the soil interaction effects within the global design of catenary riser systems is being assessed as part of STRIDE Phase 4 (STRIDE, 2000), running until March 2002.

### ACKNOWLEDGEMENT

The authors are grateful to the STRIDE JIP Participants for their permission and support in submitting this paper. The views presented in this paper are those of the authors, and may not necessarily represent those of the participants.

### STRIDE Phase III details

*Lead Engineering Contractor:* 2H Offshore Engineering

#### *Participants:*

BP	Statoil	Aker
Chevron	Texaco	Brown & Root
Conoco	TotalFinaElf	Single Buoy Moorings
Norsk Hydro	Vastar	Sofec
		Stolt Offshore

*Programme manager:* Offshore Technology Management

### REFERENCES

- Griffin O. M. (1985): "Vortex shedding from bluff bodies in shear flow: a review", Transactions of ASME, Journal of Fluid Engineering, Vol. 107.
- Humphries J. A. (1998): "Comparison between theoretical predictions for vortex shedding in shear flow and experiment", Proc. of 7th Int. Conference of Offshore Mechanics and Arctic Engineering, Houston, Texas.
- Jacobsen V., R. Bruschi, P. Simantiras, L. Vitali (1996): "Vibration Suppression Devices for Long, Slender Tubulars", Proc. of 28th Offshore Technology Conference, OTC 8156, Houston, Texas.
- MCS - Marine Computational Services (1999): "FLEXCOM-3D Non-linear Three-Dimensional Time Domain Finite Element Analysis Software", Version 5.1.
- STRIDE JIP (2000): "Phase IV Outline Proposal", Doc. No. 1300-PRP-0002, 2H Offshore Engineering Ltd, Woking, UK, [www.STRIDEJIP.co.uk](http://www.STRIDEJIP.co.uk).

- Tae-Young Chung (1987): "Vortex-Induced Vibration of Flexible Cylinders in Sheared Flows", Ph.D. Dissertation, Department of Ocean Engineering, MIT, Prof. J. Kim Vandiver, supervisor.
- Vandiver J. K. (1985): "The prediction of lock-in vibration on flexible cylinders in a sheared flow", Proc. of 17th Offshore Technology Conference, OTC 5006, Houston, Texas.
- Vandiver J. K. (1993): "Dimensionless parameters important to the prediction of vortex induced vibration of long flexible cylinders in ocean currents", Journal of Fluids and Structures, Vol. 7, 423-455.
- Vandiver J. K. (2000): "Predicting Lock-in on Drilling Risers in Sheared Flows", Proc. of Flow-Induced Vibration 2000 Conference, Lucerne, Switzerland.
- Welch P. D (1967): "The use of fast Fourier transform for the estimation of power spectra: a method based on time averaging over short, modified periodograms", Nat. Phys. Lab. (UK), Aero Rep. 384.

Logger #	Distance from top end measured along the riser [m]	(s/L)
11	0.0	0.000
03	87.3	0.073
04	138.4	0.115
05	182.2	0.151
06	195.9	0.163
07	208.1	0.173
08	235.6	0.196
09	274.4	0.228
10	323.2	0.269
12	1113.2	0.925
14	1137.6	0.946
13	1149.8	0.956

Table 1 – Data Logger Positions along the Axis of Allegheny Gas Export Line

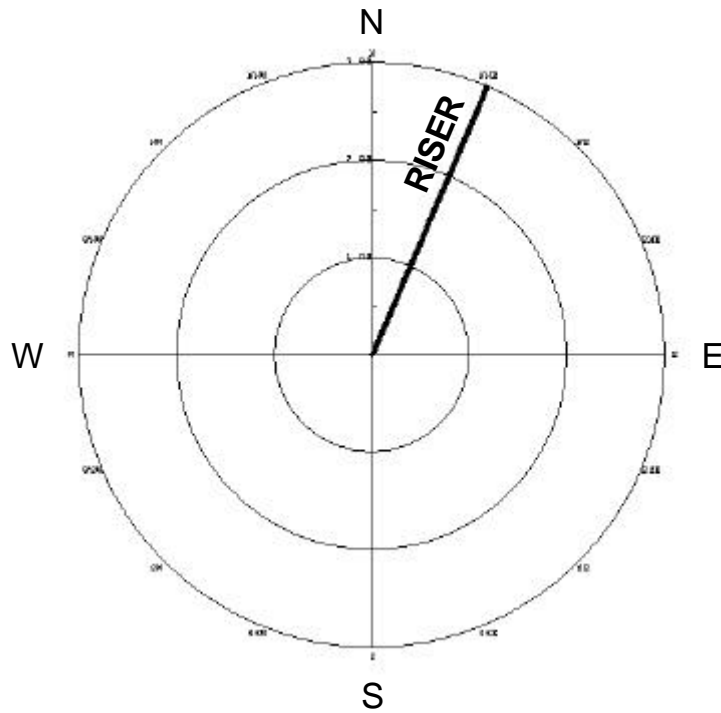


Figure 1 – Orientation of the Allegheny Gas Export Line



Figure 2 - 2H Accelerometer Data Logger

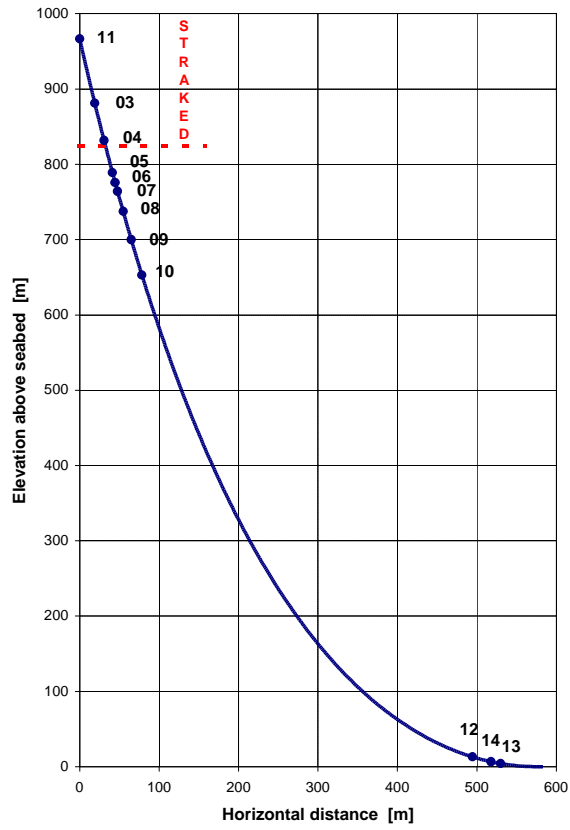


Figure 3 - Data Logger Positions along the Allegheny Gas Export Line

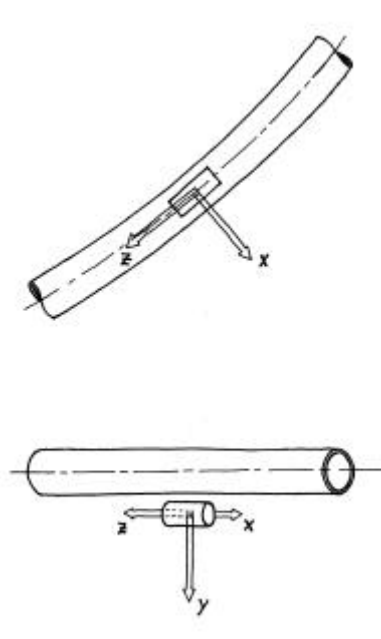


Figure 4 - Sketch of Logger Orientation

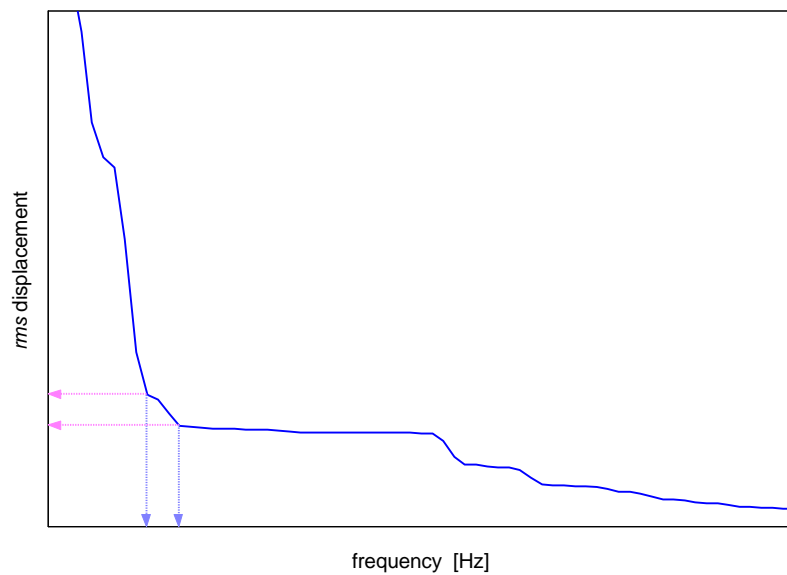


Figure 5 - Sketch of RMS Displacement vs. Cut-Off Frequency, as Evaluated through Integration of the Acceleration Power Density Spectrum

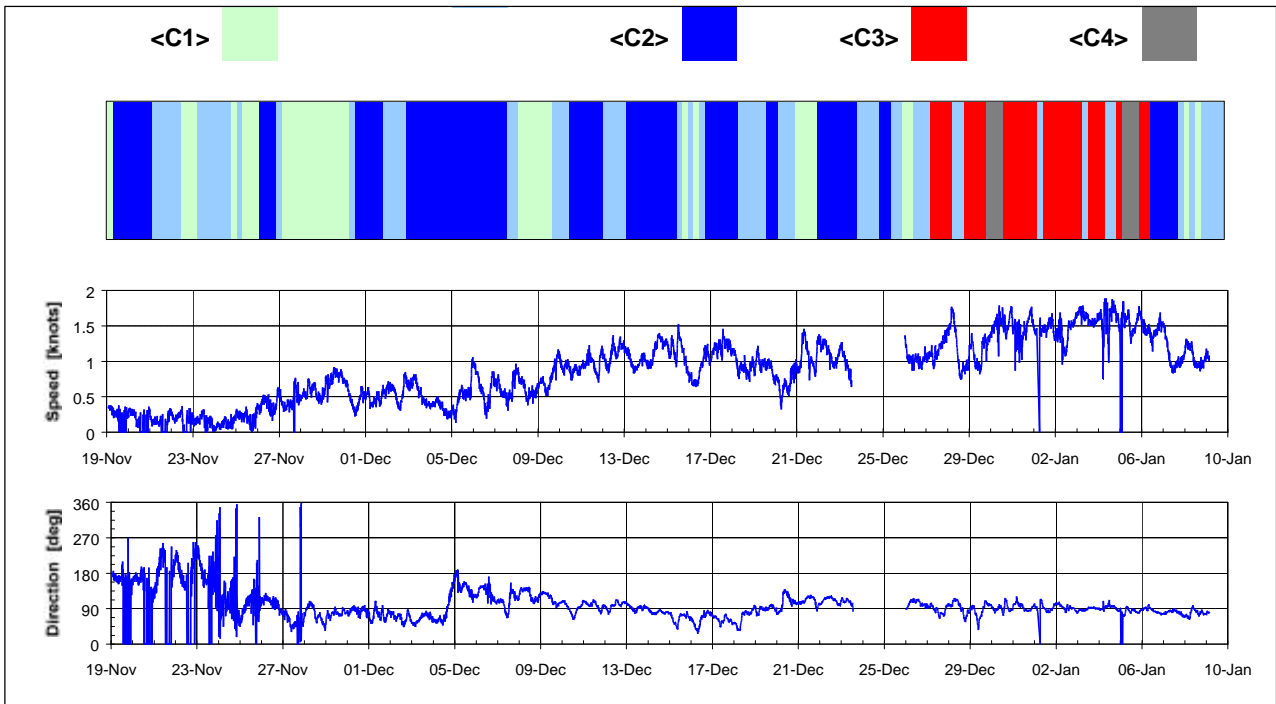


Figure 6 - Response Classification Summary

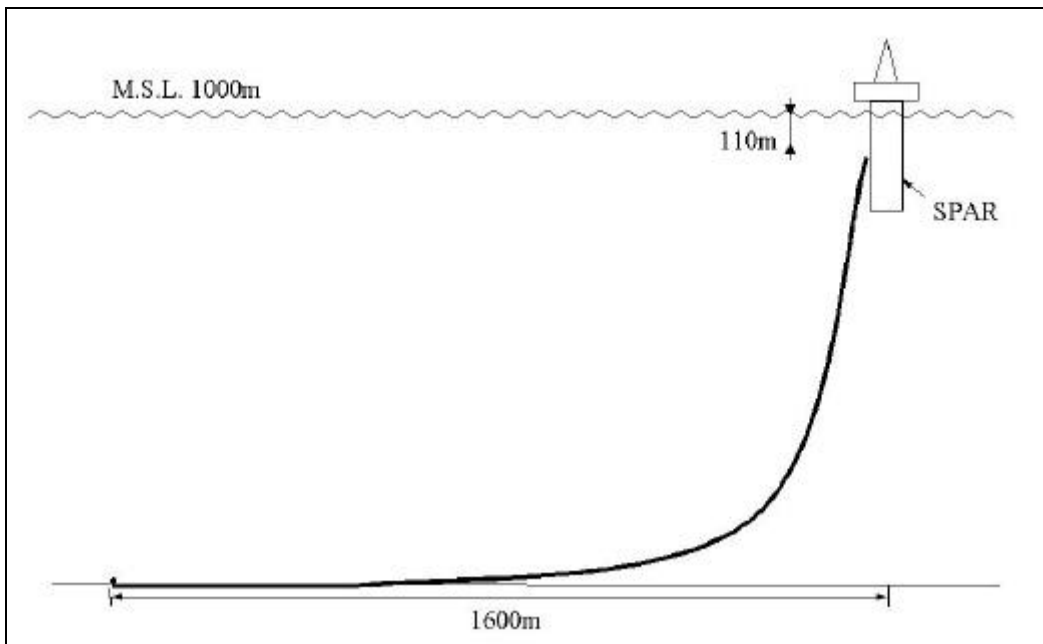


Figure 7 – Full Scale Riser Configuration

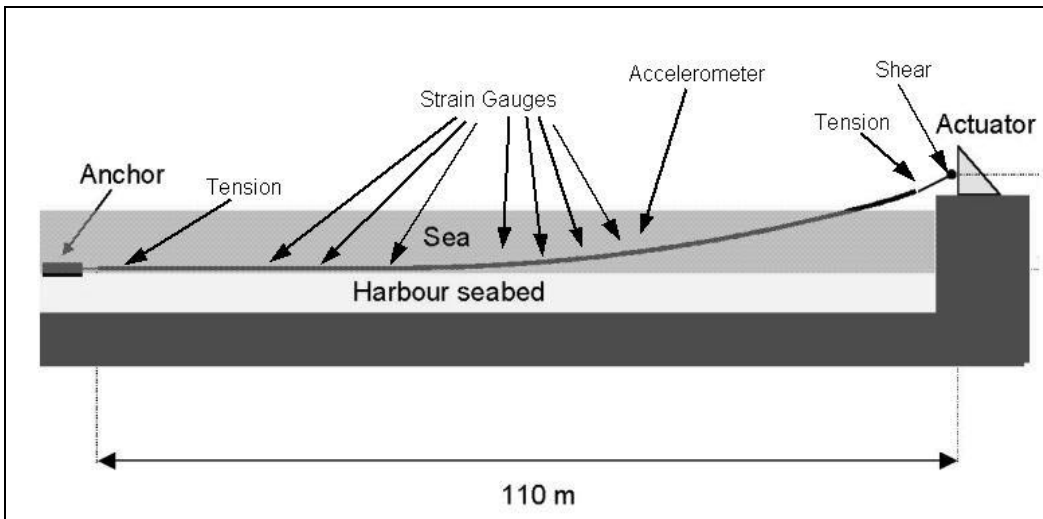


Figure 8 – Harbour Test Set-Up Schematic



Figure 9 – Harbour Test Site at Low Tide

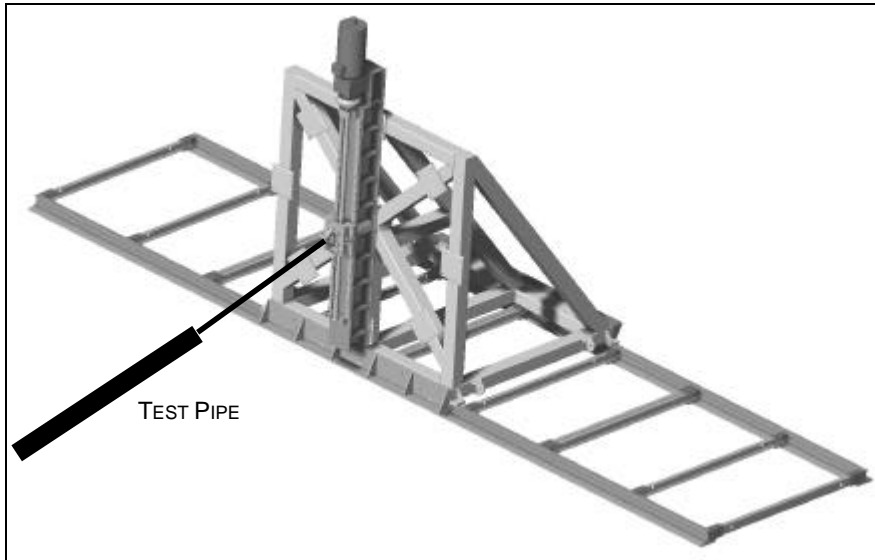


Figure 10 – Actuator Unit and Rails

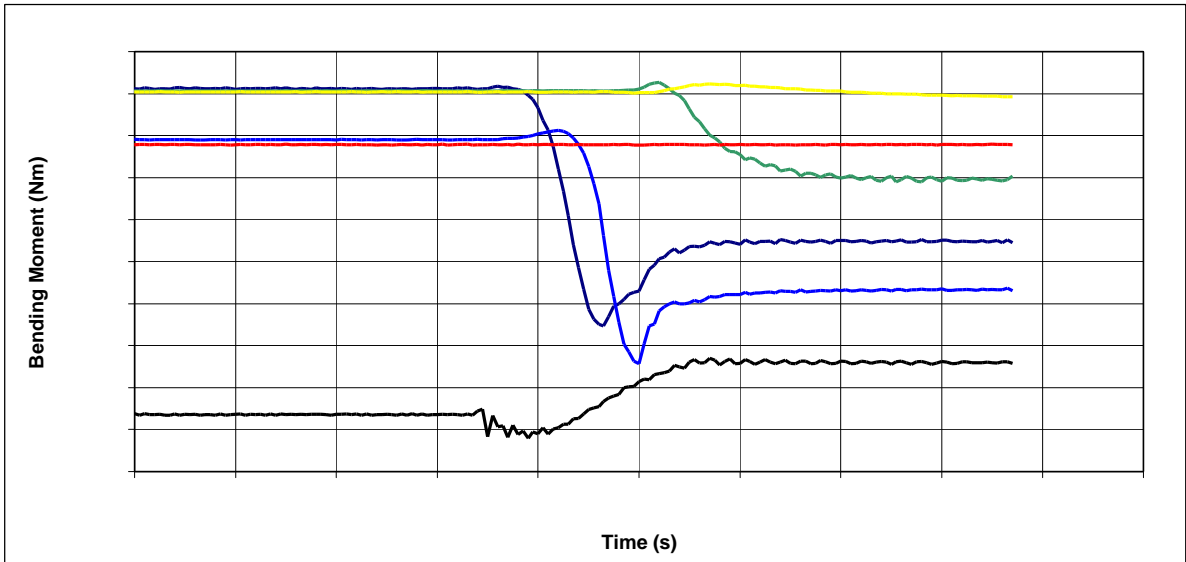


Figure 11 – Bending Strain at Different Riser Positions During a Drift Simulation

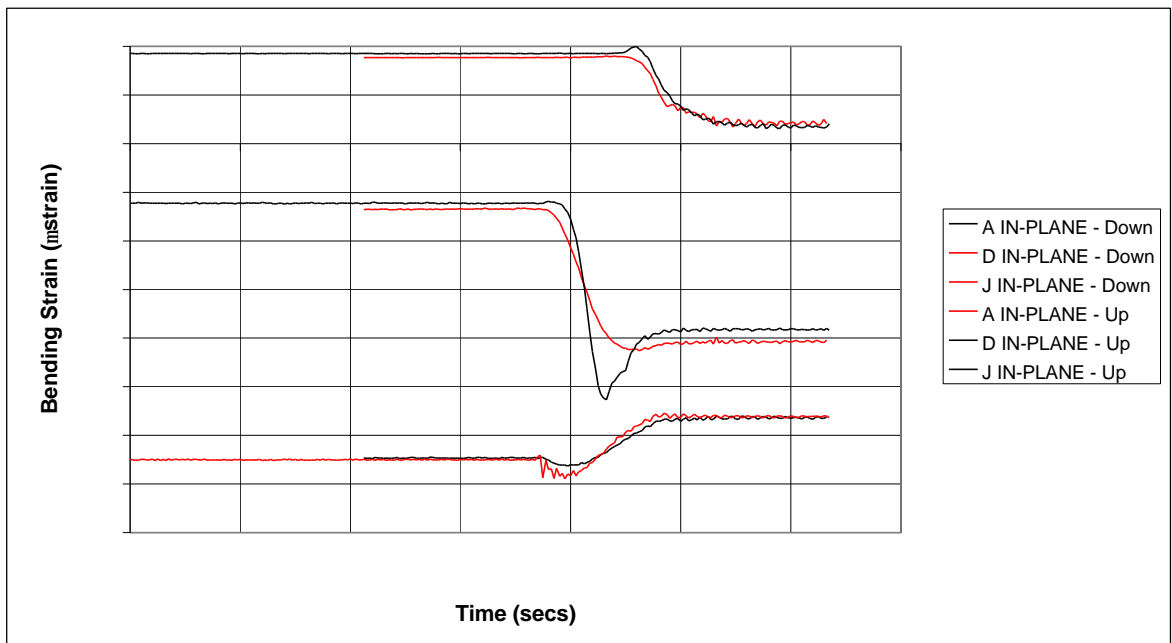


Figure 12 – Comparing Near-Far and Far-Near Bending Traces

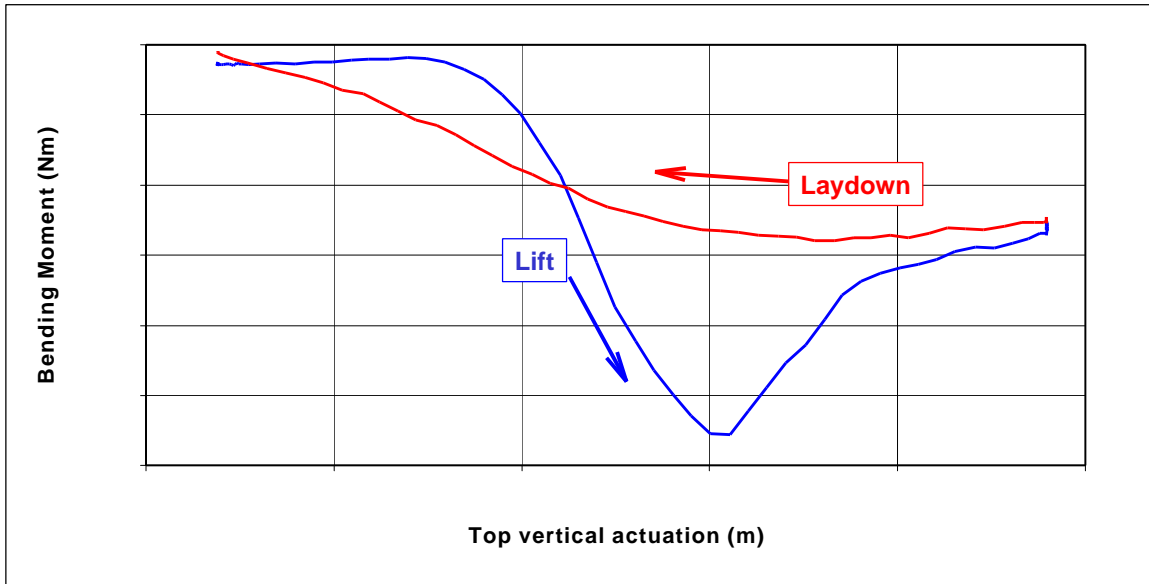
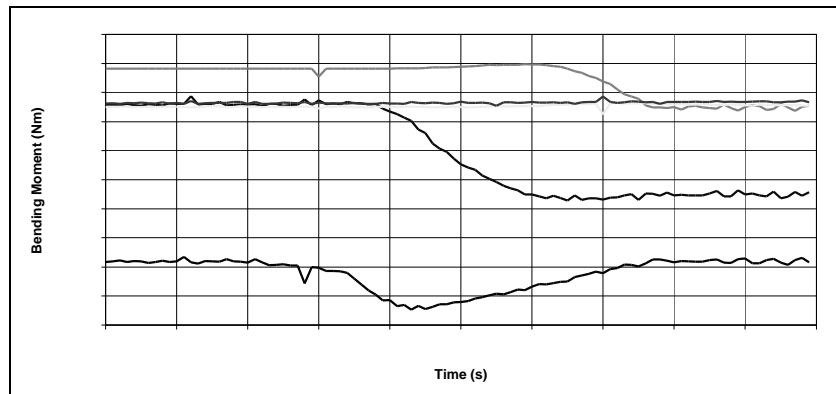
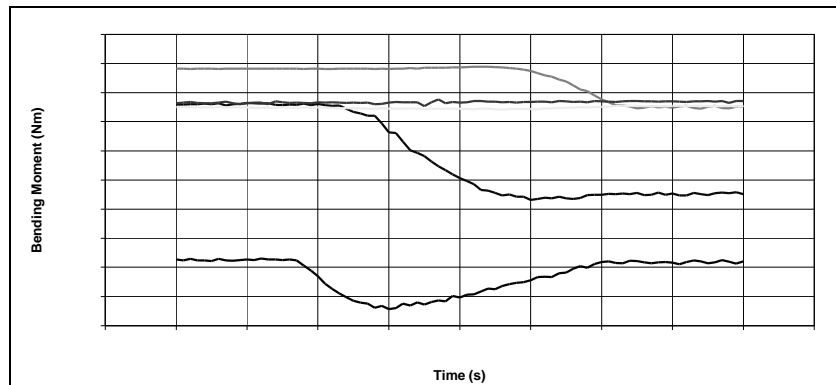


Figure 13 – Suction Peak for Fast Drift Case



(a) Lift (Near to Far)



(b) Lay-down (Far to Near)

Fig. 14 – Strain Gauge Data from Rigid Surface Tests